ω-Hydroxyemodin Limits Staphylococcus aureus Quorum Sensing-Mediated Pathogenesis and Inflammation

By: Seth M. Daly, Bradley O. Elmore, Jeffrey S. Kavanaugh, Kathleen D. Triplett, Mario Figueroa, Huzefa A. Raja, Tamam El-Elimat, Heidi A. Crosby, Jon K. Femling, Nadja B. Cech, Alexander R. Horswill, Nicholas H. Oberlies, and Pamela R. Hall.

Abstract:

Antibiotic-resistant pathogens are a global health threat. Small molecules that inhibit bacterial virulence have been suggested as alternatives or adjuncts to conventional antibiotics, as they may limit pathogenesis and increase bacterial susceptibility to host killing. Staphylococcus aureus is a major cause of invasive skin and soft tissue infections (SSTIs) in both the hospital and community settings, and it is also becoming increasingly antibiotic resistant. Quorum sensing (QS) mediated by the accessory gene regulator (agr) controls virulence factor production essential for causing SSTIs. We recently identified ω-hydroxyemodin (OHM), a polyhydroxyanthraquinone isolated from solid-phase cultures of Penicillium restrictum, as a suppressor of QS and a compound sought for the further characterization of the mechanism of action. At concentrations that are nontoxic to eukaryotic cells and subinhibitory to bacterial growth, OHM prevented agr signaling by all four S. aureus agr alleles. OHM inhibited QS by direct binding to AgrA, the response regulator encoded by the agr operon, preventing the interaction of AgrA with the agr P2 promoter. Importantly, OHM was efficacious in a mouse model of S. aureus SSTI. Decreased dermonecrosis with OHM treatment was associated with enhanced bacterial clearance and reductions in inflammatory cytokine transcription and expression at the site of infection. Furthermore, OHM treatment enhanced the immune cell killing of S. aureus in vitro in an agr-dependent manner. These data suggest that bacterial disarmament through the suppression of S. aureus QS may bolster the host innate immune response and limit inflammation.

Keywords: ω-hydroxyemodin | OHM

Article:

***Note: Full text of article below

ω-Hydroxyemodin Limits *Staphylococcus aureus* Quorum Sensing-Mediated Pathogenesis and Inflammation

Seth M. Daly,[a] Bradley O. Elmore,[a] Jeffrey S. Kavanaugh,[b] Kathleen D. Triplett,[a] Mario Figueroa,[d] Huzefa A. Raja,[d] Tamam El-Elimat,[d] Heidi A. Crosby,[b] Jon K. Femling,[c] Nadja B. Cech,[d] Alexander R. Horswill,[b] Nicholas H. Oberlies,[d] Pamela R. Hall[a]

Department of Pharmaceutical Sciences, College of Pharmacy, University of New Mexico, Albuquerque, New Mexico, USA[a]; Department of Microbiology, Carver College of Medicine, University of Iowa, Iowa City, Iowa, USA[b]; Department of Emergency Medicine, University of New Mexico Health Sciences Center, Albuquerque, New Mexico, USA[c]; Department of Chemistry and Biochemistry, University of North Carolina at Greensboro, Greensboro, North Carolina, USA[d]

Antibiotic-resistant pathogens are a global health threat. Small molecules that inhibit bacterial virulence have been suggested as alternatives or adjuncts to conventional antibiotics, as they may limit pathogenesis and increase bacterial susceptibility to host killing. *Staphylococcus aureus* is a major cause of invasive skin and soft tissue infections (SSTIs) in both the hospital and community settings, and it is also becoming increasingly antibiotic resistant. Quorum sensing (QS) mediated by the accessory gene regulator (*agr*) controls virulence factor production essential for causing SSTIs. We recently identified ω-hydroxyemodin (OHM), a polyhydroxyanthraquinone isolated from solid-phase cultures of *Penicillium restrictum*, as a suppressor of QS and a compound sought for the further characterization of the mechanism of action. At concentrations that are nontoxic to eukaryotic cells and subinhibitory to bacterial growth, OHM prevented *agr* signaling by all four *S. aureus agr* alleles. OHM inhibited QS by direct binding to AgrA, the response regulator encoded by the *agr* operon, preventing the interaction of AgrA with the *agr* P2 promoter. Importantly, OHM was efficacious in a mouse model of *S. aureus* SSTI. Decreased dermonecrosis with OHM treatment was associated with enhanced bacterial clearance and reductions in inflammatory cytokine transcription and expression at the site of infection. Furthermore, OHM treatment enhanced the immune cell killing of *S. aureus in vitro* in an *agr*-dependent manner. These data suggest that bacterial disarmament through the suppression of *S. aureus* QS may bolster the host innate immune response and limit inflammation.

Due to the widespread and seemingly inevitable development of bacterial resistance to antibiotics shortly after their introduction, there is a great need for alternatives or adjuncts to classical antimicrobials (1–3). Along with ongoing efforts to identify novel antibacterial targets, interventions that are not directly bactericidal may prove efficacious. These include approaches aimed at modifying or augmenting the host response, as well as approaches that inhibit bacterial virulence mechanisms and thus limit pathogenesis (1–3). Many pathogenic bacteria coordinate the expression of virulence factors important for invasive infection and pathogenesis through a density-dependent communication system called quorum sensing (QS) (4, 5). Therefore, approaches aimed at disrupting QS hold promise to limit pathogenesis in the host and/or serve as adjuncts to extend the utility of existing antibiotics (4, 6–10).

Skin and soft tissue infections (SSTIs) represent the majority of infections caused by *Staphylococcus aureus* (11–13), and many of the virulence factors contributing to SSTIs are globally regulated by the accessory gene regulator (*agr*) (Fig. 1A) (14–16). The *agr* system utilizes a small secreted autoinducing peptide (AIP) to activate a receptor histidine kinase, AgrC, in the bacterial cell membrane. AgrC phosphorylates the transcription factor AgrA, which in turn activates transcription at the P2 and P3 promoters of the operon. P3 activation drives the production of the effector of the operon, RNAIII, which regulates the expression of >200 virulence genes that contribute to invasive infection (14). *S. aureus* isolates have one of four *agr* alleles (*agr*-I to *agr*-IV), each encoding factors that secrete a unique AIP (AIP1 to AIP4, respectively) that is detected by a cognate AgrC histidine kinase; isolates from each allele can cause human disease (17, 18). Importantly, we and others have shown that the disruption of *agr* signaling by mu-

tagenesis, monoclonal antibodies, or host factors limits *S. aureus* infection and reduces pathogenesis (14, 19–24), demonstrating that *agr* QS is a robust target for combating invasive *S. aureus* infection.

Recently, we reported on a synthetic small-molecule inhibitor of *S. aureus* QS called savirin, providing proof of principle that small-molecule-mediated inhibition of QS can be efficacious against *S. aureus in vivo* (25). Natural products also represent a wealth of bioactive compounds, as approximately 65% of the antibacterials introduced in the last 30 years are natural products or compounds designed based on a lead natural-product pharmacophore (26). Therefore, we extended our search for inhibitors of QS to natural products and in doing so identified a series of polyhydroxyanthraquinones isolated from cultures of the fungus *Penicillium restrictum* that inhibited *S. aureus* QS (27). Among these, ω-hydroxyemodin (OHM) (Fig. 1B) demonstrated the most po-
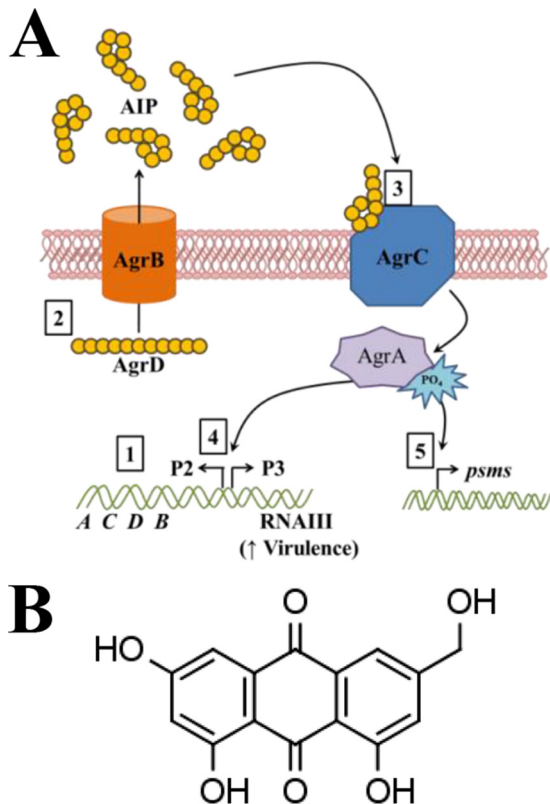
FIG 1 (A) Schematic of the *S. aureus* accessory gene regulator quorum-sensing system and structure of ω-hydroxyemodin. 1, The *agr* P2 promoter drives the expression of the four genes of the operon *agrBDCA*. 2, AgrD is a propeptide that is cyclized to form autoinducing peptide (AIP) and secreted via AgrB. AIPs from the four *agr* alleles vary in length from seven to nine amino acids, but all contain a five-membered thiolactone ring. 3, Secreted AIP binds to its cognate receptor AgrC, activating its histidine kinase function leading to the phosphorylation of AgrA. 4, AgrA binds to the divergent promoters P2 and P3 as well as the promoters for the transcription of the phenol-soluble modulin (PSM) toxins. 5, P2 drives a positive-feedback loop resulting in the upregulation of the *agr* operon, whereas P3 drives the transcription of the effector molecule RNAIII. RNAIII leads to the upregulation of virulence factors that contribute to invasive infection. (B) Structure of ω-hydroxyemodin (OHM). Molecular mass, 286.24 Da.

tent activity for inhibiting *agr*-I signaling. Therefore, we sought to characterize OHM as an inhibitor of *agr* signaling and to evaluate its efficacy *in vivo*.

Approaches aimed at augmenting the host response and those aimed at inhibiting bacterial virulence mechanisms provide alternatives to conventional antibiotic therapy. However, these two approaches are not mutually exclusive, and because many *S. aureus* virulence factors antagonize the host innate immune response, we proposed that inhibiting bacterial virulence would itself augment host defense. Specifically, we postulated that small-molecule-mediated disruption of *S. aureus* QS-dependent virulence would not only limit pathogenesis but would also reduce inflammation and result in enhanced bacterial clearance. Here, we report that OHM inhibits *S. aureus* QS by isolates from all four *agr* alleles at concentrations that are noncytotoxic to *S. aureus* or eukaryotic cells. Mechanistically, OHM inhibits *agr* activation by binding directly to AgrA and blocking binding to *agr* promoter DNA. Importantly, as predicted, OHM limits tissue damage and

inflammation and promotes bacterial clearance in a mouse model of *S. aureus* SSTI. In addition, OHM promotes the killing of *agr*⁺, but not *agr*-negative, *S. aureus* by both mouse macrophages and human polymorphonuclear leukocytes (PMNs), and it limits neutrophil lysis caused by *agr*-regulated *S. aureus*-secreted virulence factors. This is the first report of a polyhydroxyanthraquinone with *in vivo* efficacy against *S. aureus* QS-dependent virulence. In addition, these data demonstrate that antivirulence approaches can limit disease by disarming the bacteria while concurrently bolstering host innate defense.

MATERIALS AND METHODS

Ethics statements. The animal work in this study was carried out in strict accordance with the recommendations in the *Guide for the Care and Use of Laboratory Animals* (97), the Animal Welfare Act, and U.S. federal law. The protocol was approved by the Institutional Animal Care and Use Committee of the University of New Mexico Health Sciences Center. The polymorphonuclear cells were isolated from whole blood samples from consenting healthy human volunteers, according to the protocol (no. 11-005) approved by the Human Research Protections Office of the University of New Mexico institutional review board.

Bacterial strains and growth conditions. Methicillin-resistant *S. aureus* (MRSA) strain USA300 LAC (*agr*-I) was provided as a generous gift from Frank DeLeo (Rocky Mountain National Laboratories, National Institutes of Health, Hamilton, MT). *S. aureus* strains AH1677 (*agr*-I), AH430 (*agr*-II), AH1747 (*agr*-III), and AH1872 (*agr*-IV) expressing yellow fluorescent protein (YFP) under the control of the *agr*::P3 promoter were previously described (28). *Staphylococcus epidermidis* strain AH3408 (*agr*-I) expressing superfolder green fluorescent protein (sGFP) under the control of the *agr*::P3 promoter were also previously described (29). *S. aureus* strains AH3469 (AgrC wild type [WT]) and AH3470 (AgrC R238H) are described below. Unless otherwise noted, the bacteria were cultured at 37°C and 220 rpm, with at least a 5:1 air-to-culture ratio in Trypticase soy broth (TSB) (Becton, Dickinson and Company, Sparks, MD). Early exponential-phase bacteria were prepared as described previously (30). The frozen stocks were maintained at −80°C in TSB supplemented with 10% glycerol. The bacteria were enumerated by serial dilution and plating onto Trypticase soy agar containing 5% sheep blood (Becton, Dickinson and Company), followed by overnight incubation at 37°C. The limit of detection was 2 $\log_{10}$ CFU.

agr::P3 promoter activation assays. Overnight cultures of *S. aureus* *agr*::P3 reporter strains were grown in TSB supplemented with 10 μg/ml chloramphenicol (Cam). The cultures were diluted 1:250 into fresh TSB with Cam, and 100-μl aliquots were transferred to 96-well microtiter plates (Costar 3603; Corning, Tewksbury, MA) prefilled with 100 μl of medium and a 2-fold serial dilution series (200 to 0.1 μM) of OHM. OHM was purified from solid-phase cultures of *P. restrictum*, as described previously (27), and was >95% pure, as measured by ultrahigh-performance liquid chromatography (UPLC) (see Fig. S1 in the supplemental material). After mixing in the microtiter plate, the effective dilution was 1:500, and the final OHM concentration ranged from 100 to 0.05 μM, with a final dimethyl sulfoxide (DMSO) concentration of 0.1% (vol/vol) in all wells. Four dilution series were prepared for each reporter; in addition, 4 mock DMSO dilution series were included for each reporter strain. The microtiter plates were incubated at 37°C with shaking (1,000 rpm) in a Stuart SI505 incubator (Bibby Scientific, Burlington, NJ) with a humidified chamber. Fluorescence (top reading of 493 nm excitation, 535 nm emission, and gain of 60) and optical density at 600 nm (OD₆₀₀) readings were recorded at 30-min increments using a Tecan Systems (San Jose, CA) Infinite M200 plate reader.

S. epidermidis AH3408 (*agr*-I::P3-sGFP) was cultured overnight in TSB supplemented with 10 μg/ml erythromycin (Erm). To collect exogenous *S. epidermidis* AIP1 peptide, the spent medium was centrifuged at 3,000 × *g*, passed through a 0.2-μm HT Tuffryn membrane (Pall, Port Washington, NY), and stored at −20°C until use. An overnight culture of

AH3408 was diluted 1:200 into 500 μl of TSB (broth) or TSB with 10% spent medium containing 5 μg/ml OHM or DMSO (vehicle). The cultures were incubated for 24 h at 37°C, centrifuged, and resuspended in 10% formalin fixative for 1 min. The cultures were washed twice by centrifugation and resuspended in phosphate-buffered saline (PBS). The mean channel fluorescence (MCF) of sGFP was analyzed using an Accuri C6 flow cytometry system (BD Biosciences, San Jose, CA). The data were normalized to the broth cultures containing no exogenous AIP1.

Quantitative PCR. For transcriptional quantification of mouse mRNA, 2.25-cm^2 sections of skin including and surrounding the abscess were excised, minced, and stored in RNA*later* (Qiagen, Valencia, CA) at −20°C until use. mRNA was purified using the RNeasy kits (Qiagen), and cDNA was generated using a high-capacity RNA-to-cDNA kit (Applied Biosystems, Foster City, CA). Quantitative PCR was performed using an ABI 7900HT real-time PCR system with TaqMan Gene expression master mix, according to the manufacturer's directions (Applied Biosystems). Predesigned primer and probe sets (Integrated DNA Technologies, Coralville, IA) were used for the quantitation of mouse *il-6*, *il-1β*, *tnfα*, *nlrp3*, and *hprt*. The data are represented as the fold increase relative to *hprt* compared to that in uninfected tissue.

For the quantification of *S. aureus* gene transcription, 500-μl cultures at 2×10^7 CFU/ml of LAC and/or LACΔ*agr* were grown in TSB at 37°C, with aeration, for the indicated times with 50 nM exogenous AIP1 (Biopeptide Co., Inc., San Diego, CA) and treatments (vehicle versus OHM), as indicated in the appropriate figure legends. The bacteria were stored at −20°C in RNAprotect cell reagent, according to the manufacturer's recommendations (Qiagen), until the RNA was purified as previously described (25). cDNA generation and quantitative PCR (qPCR) were performed as described above for eukaryotic qPCR. The primer and probe sets for the quantification of the *S. aureus* genes are listed in Table S1 in the supplemental material.

Rabbit red blood cell lysis assay. The assay was performed as previously described (31). Briefly, LAC was cultured in 5 ml of TSB for 8 h with the indicated treatments, centrifuged, and the supernatants were filtered through a 0.2-μm HT Tuffryn membrane (Pall). Serial 2-fold dilutions of the supernatant were incubated at 37°C for 1 h in a 4% solution of rabbit red blood cells (rRBCs). Lysis was assessed spectrophotometrically at OD$_{450}$. The data were analyzed by nonlinear regression fit to a four-parameter logistic curve and represented as the HA$_{50}$, which equals 1/the dilution required for 50% complete lysis.

AgrC constitutive reporter assay. The *agrBDCA* operon was amplified from strain LAC using the primers AgrB+RBS 5′–KpnI (GTTGGTA CCCAGTGAGGAGAGTGGTGTAAAATTG) and AgrA 3′-SacI (GTTGA GCTCCTTATTATATTTTTTTAACGTTTCTCACCGATG) and ligated into pRMC2 (32). To make a variant with constitutive AgrC activity, we chose the AgrC R238H mutation, which was previously shown to have similar activity in the presence and absence of the AIP2 inhibitor and maximal activity in the absence of AIP1 (33). The AgrC R238H variant was generated by the QuikChange (Agilent Technologies) site-directed mutagenesis method, using the primers AgrC R238H fwd (CAACGAAA TGCGCAAGTTCCATCATGATTATGTCAATATC) and AgrC R238H rev (GATATTGACATAATCATGATGGAACTTGCGCATTTCGTTG). To build a destination strain for assessing alpha-hemolysin production, we selected an *agrC* transposon mutant (NE873) from the Nebraska Transposon Mutant Library (34) and integrated the pLL29 plasmid at the phage 11 attachment site to confer tetracycline resistance (35). The above-described pRMC2 constructs were transformed into this strain to make reporters AH3469 (AgrC WT) and AH3470 (AgrC R238H). To test OHM, AH3469 and AH3470 were grown overnight with 10 μg/ml Cam and were diluted 1:500 into 5 ml of fresh medium with 10 μg/ml Cam and 0.025 μg/ml anhydrotetracycline. AIP2 control, OHM, or DMSO (vehicle) was added to each strain at the concentrations indicated. The cultures were grown at 37°C and shaken at 220 rpm for 6.5 h. The bacteria were pelleted by centrifugation, and the alpha-hemolysin-containing supernatants were passed through a 0.2-μm HT Tuffryn membrane (Pall). Rabbit red

blood cell lysis assays were conducted as above but with an rRBC concentration of 1% and 25% supernatant (vol/vol) to yield complete lysis. The values are presented as the mean relative lysis compared to that with vehicle treatment.

Eukaryotic cytotoxicity. A549, HEK293, or HepG2 cells were seeded in a 96-well tissue culture plate at 2.5×10^4 cells per well and incubated at 37°C with 5% CO$_2$. XTT [2,3-Bis(2-methoxy-4-nitro-5-sulfophenyl)-2H-tetrazolium-5-carboxanilide] and phenazine methosulfate (PMS) were purchased from Sigma-Aldrich (St. Louis, MO). The XTT assay was previously described (36). After 24 h, the spent medium was removed, and fresh medium containing the indicated drug concentrations or vehicle was added to the cells and incubated for an additional 24 h. To avoid potential interference with the absorbance readings due to the red color of OHM, drug-containing medium was replaced with 100 μl of 0.3 mg/ml XTT with 0.015 mg/ml PMS in Hanks' balanced salt solution (HBSS) and incubated for 1 h. Cell viability was assessed by the metabolic reduction of tetrazolium measured at OD$_{490}$. The data are presented as the percentage of viable cells compared to that in the vehicle control.

EMSA and flow cytometry-based AgrA$_C$ promoter binding assays. *Escherichia coli* expressing the AgrA C-terminal DNA binding domain (AgrA$_C$) along with a 6-histidine tag was generously provided by Chuan He (University of Chicago, Chicago, IL) and purified as previously described (37). Electrophoretic mobility shift assays (EMSA) were performed as previously described (25), with purified AgrA$_C$ and a*gr* P2 promoter, and a 16-bp duplex DNA probe with a 3′ 6-fluorescein (P2-FAM) (Integrated DNA Technologies, Coralville, IA). The duplex DNA contained the high-affinity LytTR binding site located in both *agr* P2 and P3 promoters (38). Briefly, 2 μM AgrA$_C$ was incubated for 10 min at room temperature (RT) with vehicle or the indicated concentrations of OHM in Tris-acetate-EDTA (TAE) buffer with 10 mM dithiothreitol (DTT). Next, 20 ng of P2-FAM DNA probe was added and incubated for an additional 10 min. The reaction mixtures were loaded onto a 10% PAGE gel and run at 50 V in the dark for 20 min. DNA migration was assessed by imaging on a FluorChem R system (ProteinSimple, Santa Clara, CA).

For the flow-based AgrA$_C$ promoter binding assays, AgrA$_C$ was biotinylated (AgrA$_C$-BTN) using a Thermo Scientific EZ-Link sulfo-NHS-LC-biotin kit (Thermo Scientific, Rockford, IL), according to the manufacturer's directions. AgrA$_C$-BTN was immobilized on 1-μm-diameter Dynabeads MyOne streptavidin T1 (Life Technologies, Grand Island, NY) (AgrA$_C$-SA), and the beads were suspended in PBS. DNA probe (P2-FAM) was added at a final concentration of 1.6 μM, along with equimolar competing unlabeled P2, vehicle control, or OHM at the indicated concentrations. OHM-mediated inhibition of AgrA$_C$-SA binding to DNA probe was measured as decreased mean channel fluorescence (MCF) compared to that of the vehicle control using an Accuri C6 flow cytometry system (BD Biosciences).

***In silico* docking on AgrA$_C$.** *In silico* docking calculations were performed using the Macintosh binary executable of AutoDock Vina (39). OHM was docked onto the B subunit of the AgrA$_C$ crystal structure (RSCB Protein Data Bank [www.pdb.org], PDB ID 4G4K) (40, 41) stripped of heteroatoms. The search box was restricted to the C-terminal region of AgrA$_C$, as described for 9H-xanthene-9-carboxylic acid (40). Based on initial observations suggesting that OHM bound to the pocket between the side chains of His200, Agr218, Tyr229, and Val232, additional calculations were run in which the size of search box was varied and the side-chain torsion angles for different combinations of residues in the region were allowed to be flexible. The reported docking solution was obtained by allowing flexibility in the side chain torsion angles for His200, Agr218, Tyr229, and Val232 and by using a search box that was large enough to include both the pocket bounded by the side chains of His200, Agr218, Tyr229, and Val232 and the groove between Val232 and Lys236. Molecular modeling images were prepared using PDB ID 3BS1 and PyMOL (PyMOL molecular graphics system, version 1.5.0.4; Schrodinger, LLC).

Surface plasmon resonance analysis. To overcome the potential interference for the oxidative inactivation of $AgrA_C$ during surface plasmon resonance (SPR) analysis, the oxidation-resistant C199S mutation was introduced into the $AgrA_C$ expression construct, as previously described (37), using the QuikChange II XL kit (Agilent Technologies). His-tagged $AgrA_C$-C199S was purified as described previously (25) but without the addition of Tris(2-carboxyethyl)phosphine (TCEP) or DTT during purification.

SPR binding and kinetics analyses were performed on a Biacore X100 instrument (GE Healthcare, Pittsburgh, PA) and evaluated with Biacore X100 evaluation software (version 1.0). His-tagged $AgrA_C$-C199S was immobilized at 10 µg/ml in PBS on a nitrilotriacetic acid (NTA) biosensor with the NTA reagent kit (GE Healthcare). For binding studies, OHM (analyte) was dissolved in running buffer (PBS, 5% DMSO [pH 9]) and applied at a flow rate of 30 µl/min with a 180-s contact time and 300-s dissociation time. The data were fit to a 1:1 binding model after the subtraction of blank injections and the removal of injection spikes from the sensorgrams. NTA biosensor chips were regenerated with the following sequence: two 60-s washes with 350 mM EDTA, a 60-s wash with PBS, and a 60-s wash with 500 mM imidazole, followed by a final 60-s wash with PBS. The analyses were performed at 25°C.

Mouse model of skin and soft tissue infection. The mouse model of skin and soft tissue infection was previously described and was implemented with minor modifications (42). Early exponential-phase *S. aureus* strain LAC was diluted into USP-grade saline (Braun, Irvine, CA) to deliver 5×10^7 to 7×10^7 CFU per mouse. Aliquots of OHM were diluted in 0.5% hydroxypropylmethylcellulose (HPMC) (pH 11) to deliver 0.2 mg/kg per mouse (~5 µg). The mice were anesthetized with 3% isoflurane at 3 liters/min. The bacteria and OHM were mixed 1:1 immediately before subcutaneous injection into the right flank, at a total volume of 50 µl. The mice were weighed prior to infection and every day postinfection. Additionally, the injection sites were photographed daily to determine the abscess and ulcer areas with ImageJ analysis (43). On day three or day seven postinfection, each mouse was euthanized by CO_2 asphyxiation, and a 2.25-cm^2 section of skin surrounding the abscess was excised. The tissue was mechanically homogenized and serially plated on sheep blood agar to determine the bacterial burden. The tissue homogenates were stored at −80°C until they were rapidly defrosted at 37°C for cytokine analysis. On day 3 postinfection, the homogenate was centrifuged at $12,500 \times g$ for 10 min and the clarified supernatant analyzed with a custom-designed multiplex assay (Merck KGaA, Darmstadt, Germany) using a BioPlex 200 with BioPlex Manager software (Bio-Rad, Hercules, CA). The abscess tissues collected for hematoxylin and eosin (H&E) staining were fixed overnight in 10% formalin and embedded in paraffin. Five-micrometer sections were then stained with H&E and imaged using an Olympus IX70 microscope (Olympus, Center Valley, PA).

Alpha-hemolysin quantification. For the detection of alpha-hemolysin (Hla) in abscess tissue homogenates by Western blot assay, clarified homogenates were rapidly thawed and an aliquot electrophoresed on a 16% Tris-glycine SDS-PAGE gel (Life Technologies, Grand Island, NY) before transfer to a polyvinylidene fluoride membrane. The membranes were blocked for 1 h at RT, using TBST (20 mM Tris [pH 7.5], 150 mM NaCl, 0.1% Tween 20) with 5% nonfat dry milk. Hla was detected using anti-Hla antibody (ab15948; Abcam, Cambridge, MA) at a 1:1,000 dilution and alkaline phosphatase-conjugated secondary antibody. The immunoreactive bands were developed with nitroblue tetrazolium (NBT)/5-bromo-4-chloro-3-indolyl-phosphate (BCIP) (Thermo Scientific) and intensity measured using a FluorChem R system and the AlphaView software (ProteinSimple). Relative intensity was calculated as the measured intensity divided by the total protein concentration based on absorbance at 280 nm.

Mouse macrophage killing of *S. aureus*. Murine macrophage cells (RAW 264.7) were maintained at 37°C in 5% CO_2 in high-glucose Dulbecco's modified Eagle's medium (DMEM) supplemented with 10% fetal bovine serum (FBS), 2 mM L-glutamine, 10 mM HEPES, with 100 U/ml penicillin and 100 µg/ml streptomycin. Twenty-four hours prior to the experiments, the RAW cells were washed with PBS and the medium replaced with DMEM, as described above but with 2% FBS without antibiotics. Early exponential-phase LAC or LACΔagr was cultured in 3 ml of TSB at 2×10^7 CFU/ml at 37°C, with aeration for 5 h, with 50 nM exogenous AIP1 (Biopeptide Co.) and 5 µg/ml OHM or DMSO (vehicle). The bacteria were centrifuged, washed in PBS, sonicated, and suspended at 1×10^8 to 2×10^8 in DMEM but with 1% FBS without antibiotics. The bacteria were opsonized overnight at 4°C with rabbit anti-*S. aureus* IgG at 100 µg/ml (catalog no. YVS6881; Accurate Chemical & Scientific Co., Westbury, NY). The RAW cells were washed with PBS and suspended at 2×10^7 cells/ml in DMEM with 1% FBS without antibiotics and combined with opsonized bacteria at a multiplicity of infection (MOI) of 1:1. The cells were centrifuged at $500 \times g$ for 3 min to initiate contact and incubated at 37°C in 5% CO_2 for 1 h to allow phagocytosis. Lysostaphin (catalog no. L-0761; Sigma-Aldrich) was added at 2 µg/ml for 15 min to kill extracellular bacteria and then removed by centrifugation and replacement with fresh medium. Half of the samples were immediately processed for CFU determination, and the other half were incubated for an additional 4 h before CFU enumeration. Intracellular bacteria were enumerated by preliminary dilution into PBS–0.1% Triton X-100, followed by sonication and plating onto blood agar.

Human PMN assays. PMNs were purified from normal healthy venous blood, as described by Nauseef (44). The purified PMNs were suspended in HBSS without divalent cations at ≤3×10^7 cells/ml and kept on ice until use.

PMN phagosomal killing of *S. aureus* was conducted as previously described, with the following alterations (45). Prior to opsonization, early exponential-phase LAC or LACΔagr was cultured in 3 ml of TSB at 2×10^7 CFU/ml at 37°C, with aeration for 5 h, with 50 nM exogenous AIP-I (Biopeptide Co.) and 5 µg/ml OHM or DMSO (vehicle). The bacteria were centrifuged, washed in PBS, and opsonized at 5×10^6 CFU/ml in HBSS, with divalent cations supplemented with 20 mM HEPES, 1% human serum albumin (HSA), and 10% pooled human serum. Following a 20-min incubation with tumbling at 37°C, the bacteria were pelleted, washed in PBS, and resuspended in HBSS with divalent cations supplemented with 20 mM HEPES. The PMNs and opsonized bacteria were combined at an MOI of 1:1 and incubated for 10 min at 37°C. The extracellular bacteria were removed by centrifugation at $500 \times g$ for 5 min, followed by the resuspension of infected PMNs in HBSS with divalent cations supplemented with 20 mM HEPES and 1% HSA. The infected PMNs were incubated at 37°C for 120 min, and the aliquots were removed at 0, 30, 60, and 120 min. The aliquots were diluted into PBS–0.1% Triton X-100 to lyse the cells and then serially diluted and plated on blood agar for CFU enumeration.

The lysis of PMNs by the *S. aureus* supernatant was conducted as previously described, with minor modifications (25). Briefly, LAC was cultured in 3 ml of TSB for 5 h with 5 µg/ml OHM or vehicle, centrifuged, and the supernatants were filtered through a 0.2-µm HT Tuffryn membrane (Pall). The supernatants were stored at −80°C and thawed on ice prior to use. The PMNs were washed with PBS and resuspended in RPMI supplemented with 10 mM HEPES and 1% HSA. PMNs at a density of 3×10^6 cells/ml in 100 µl were added to 100 µl of RPMI, RPMI with 10% TSB (vol/vol), or RPMI with 10% *S. aureus* supernatant prepared as described above. The PMNs were incubated at 37°C and 5% CO_2 for 2 h. Following incubation, the supernatants were collected by centrifugation at $3,000 \times g$ for 5 min and assessed for lactate dehydrogenase (LDH) release, according to the manufacturer's specifications (CytoTox 96 nonradioactive cytotoxicity assay; Promega Co., Madison, WI). Triton X-100 was added at a final concentration of 0.1% (vol/vol) as a 100% lysis control, while cell-free RPMI with 5% TSB served as a blank. The data are normalized to 100% lysis control.

Statistical analysis. Statistical evaluations were performed using GraphPad Prism version 5.04. The *in vitro* data were analyzed by the two-tailed Student's *t* test, and the *in vivo* data were analyzed by the Mann-
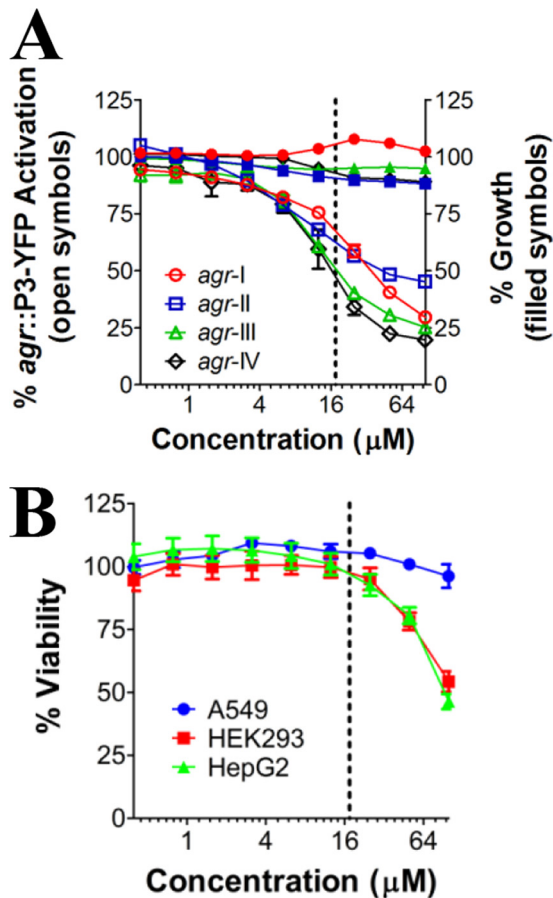
FIG 2 ω-Hydroxyemodin inhibits *S. aureus* quorum sensing by all four *agr* alleles. (A) Effect of OHM on *agr*::P3 promoter activation (open symbols) and cell growth (closed symbols), measured by flow cytometry and OD_{600}, respectively, for *agr*-I (red circles), *agr*-II (blue squares), *agr*-III (green triangles), and *agr*-IV isolates (black diamonds). (B) Percent cell viability of A549 (blue circles), HEK293 (red squares), and HepG2 (green triangles) cells measured by XTT assay after 24 h of incubation with the indicated concentrations of OHM. The dashed vertical lines indicate the concentration used for the *in vitro* assays. Data are shown as means ± SEM. The experiments were performed in triplicate or quadruplicate.

Whitney U test for nonparametrics. The results were considered significantly different at a *P* value of <0.05.

RESULTS

ω-Hydroxyemodin is a universal inhibitor of *S. aureus* quorum sensing. Our original report focused on OHM inhibition of QS using an *S. aureus* strain derived from the USA300 *agr*-I isolate LAC (27). However, isolates from all four *agr* alleles contribute to disease in humans. Therefore, to be of maximum utility, a QS inhibitor must antagonize QS by all four *agr* alleles. To address this, we assessed the ability of OHM to inhibit quorum sensing by isolates of all four *agr* types using reporter strains expressing yellow fluorescent protein (YFP) under the control of the *agr*::P3 promoter. OHM inhibited QS by all four *agr* types at concentrations that do not impact bacterial growth (Fig. 2A). As expected based on the inhibition of *agr*::P3 promoter activation, OHM decreased the transcription of the *agr* effector RNAIII and *agr*-regulated virulence factors, including phenol-soluble modulin alpha (*psmα*) and alpha-hemolysin (*hla*) (see Fig. S2A in the supple-

mental material). OHM also inhibited the production of Hla, as demonstrated by the red blood cell lysis assay (see Fig. S2B in the supplemental material). Importantly, at concentrations required for *agr* inhibition, OHM was nontoxic to human alveolar (A549), kidney (HEK293), and hepatocyte cell lines (Fig. 2B). Therefore, these data demonstrate that at concentrations that are noncytotoxic to eukaryotic cells, OHM is a universal inhibitor of *S. aureus* QS.

ω-Hydroxyemodin antagonizes AgrA function. The ability of OHM to antagonize QS by all *S. aureus agr* alleles pointed to a target that is well conserved in the system. Therefore, we first focused on AgrC, the receptor histidine kinase activated by AIP binding. To determine whether OHM disrupted AgrC activation, we tested OHM for the inhibition of *agr*-mediated Hla expression determined by the lysis of rabbit RBCs, using an *agr*-I isolate expressing constitutively active AgrC (R238H [33]). Whereas the addition of inhibitory AIP (AIP2) reduced Hla expression by *S. aureus* expressing wild-type (WT) but not constitutively active AgrC, OHM inhibited Hla expression by both isolates (Fig. 3A). These results support a mechanism of action whereby OHM intracellularly inhibits *agr* signaling, downstream of AgrC activation.

The response regulator AgrA functions downstream of AgrC, and we and others have shown that small molecules that target AgrA disrupt QS (25, 40). Therefore, to further address the mechanism of action of OHM, we evaluated potential OHM binding sites on the crystal structure of the C-terminal AgrA DNA binding domain ($AgrA_C$) (39, 40). The most favorable binding site for OHM was near the $AgrA_C$-DNA interface (Fig. 3B). Docking studies positioned OHM in a pocket between the side chains of H200 and Y229, with Y229 recently identified as a major contributor to maximal AgrA activity (46), and three residues, R218, S231, and V232, which make direct interactions with bound DNA in the AgrA-DNA crystal structure (38). Given this, together with observations that OHM is within hydrogen bonding distance of R218 and that naturally occurring mutations at R218 result in *agr*-negative phenotypes (47), we predicted that OHM would inhibit AgrA binding to promoter DNA. To test this, we expressed $AgrA_C$ and measured binding to fluorescently labeled duplex *agr* promoter DNA encompassing the high-affinity binding site located in the *agr* P2 and P3 promoters (P2-FAM). As expected, OHM demonstrated a dose-dependent inhibition of $AgrA_C$ binding to *agr* promoter DNA by an electrophoretic mobility shift assay (EMSA) (see Fig. S3A in the supplemental material). In addition, we developed a bead-based assay to measure transcription factor binding to target DNA using flow cytometry. Biotinylated $AgrA_C$ was immobilized on streptavidin beads (SA beads), and the binding to promoter DNA was measured by flow cytometry. As expected, OHM again demonstrated a dose-dependent inhibition of $AgrA_C$ binding to *agr* promoter DNA (Fig. 3C). Furthermore, OHM bound directly to immobilized $AgrA_C$, as shown by surface plasmon resonance (SPR) analysis (Fig. 3D). Finally, because the amino acid sequence in the predicted OHM binding site of *S. aureus* AgrA is highly conserved with that of *S. epidermidis* AgrA, we postulated that OHM would also inhibit *agr* signaling by *S. epidermidis*. As expected, OHM significantly inhibited *agr* activation by *agr*-I *S. epidermidis* (see Fig. S3B in the supplemental material). Together, these data strongly suggest that OHM inhibits *agr* signaling by binding to AgrA and blocking AgrA function.

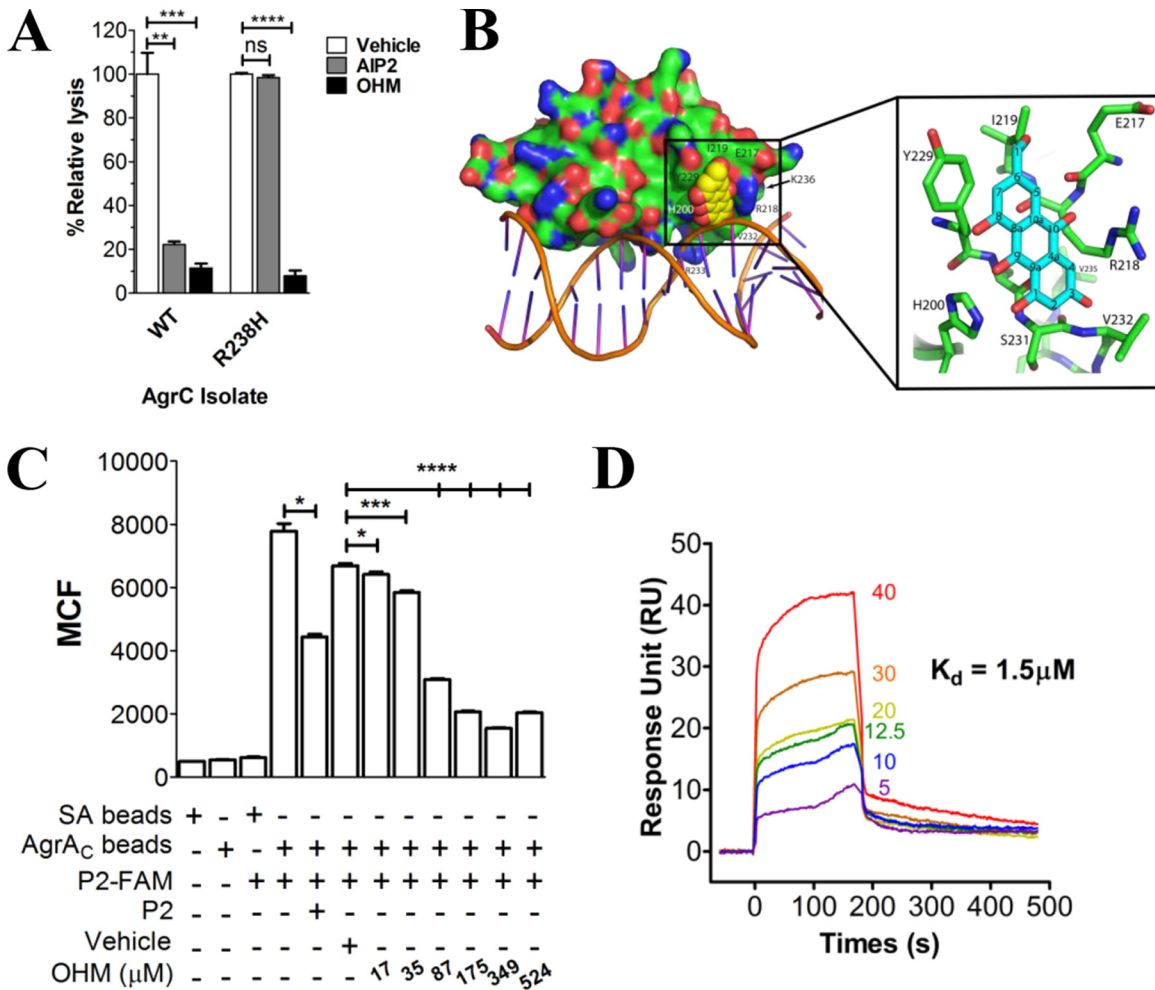To begin to address the specificity of OHM for *agr* inhibition,

FIG 3 ω-Hydroxyemodin inhibits AgrA binding to promoter DNA. (A) Effect of OHM on *agr*::P3 promoter activation assessed by rabbit red blood cell lysis for AgrC-WT isolate AH3469 and AgrC-R238H isolate AH3470. The data are the mean relative lysis ± standard error of the mean (SEM) compared to the vehicle control. The experiments were performed in triplicate. ns, not significant. (B) Space-fill model of AgrA$_C$ showing potential binding site for OHM. Inset, ball-and-stick representation of OHM binding site. (C) Flow cytometric bead-based assay to determine the effect of OHM on the binding of P2-FAM to biotinylated AgrA$_C$ immobilized on streptavidin beads (SA beads). Unlabeled P2 binding to immobilized AgrA$_C$ in competition with P2-FAM was included as a specificity control. The data are the mean ± SEM ($n = 3$). (D) Surface plasmon resonance analysis of OHM binding to 6-His-tagged AgrA$_C$-C199S immobilized on a nitrilotriacetic acid biosensor. The 50% inhibitory concentration (IC$_{50}$) was calculated as described in Materials and Methods. K_d, dissociation constant. *, $P < 0.05$; **, $P < 0.01$; ***, $P < 0.001$; ****, $P \leq 0.0001$ by Student's *t* test.

we used qPCR to evaluate the effects of OHM on transcription of a series of *agr*- and non-*agr*-regulated genes involved in virulence, the stress response, metabolism, and drug efflux and resistance (14, 25, 48, 49) (Table 1; see also Fig. S4 in the supplemental material). With respect to virulence genes, OHM treatment resulted in a slight yet nonsignificant increase in the transcription of *spa*, which encodes protein A and is negatively regulated by *agr* (14). In contrast, the expression of the enterotoxin gene *set7* decreased with OHM in LAC but not LACΔ*agr*, and OHM had no effect on the expression of the *saeR* component of the SaeRS virulence regulator. Likewise, the transcription of genes involved in the stress response (*asp23*, *crtM*, and *clpB*) was not altered by OHM, suggesting that OHM does not induce a general stress response in LAC under the conditions tested (50–54). Among the metabolism genes examined, OHM had no significant effect on the transcription of the genes involved in electron transport (*atpG* and *sdhA*). However, OHM treatment significantly decreased the

transcription of *murQ*, an *N*-acetylmuramic acid 6-phosphate lyase, in both LAC and LACΔ*agr*. Although this protein, which is involved in cell wall recycling, is dispensable for growth in *E. coli* (55–57), its contribution to the growth of Gram-positive pathogens is less clear. However, the absence of bactericidal or bacteriostatic effects with OHM treatment suggests that MurQ is not required for growth under the conditions tested. In addition, OHM treatment did not increase the transcription of genes examined for their potential to contribute to drug efflux or resistance. Therefore, although there are some non-*agr* effects, these results suggest that OHM is not a general inhibitor of transcription or energetics, nor is it a general inducer of drug efflux. Furthermore, together with the above demonstrations of (i) OHM-mediated *agr* inhibition in a whole-cell assay, (ii) OHM-mediated inhibition of AgrA$_C$ binding to *agr* promoter DNA by both EMSA and bead-based assay, and (iii) the direct binding of OHM to AgrA$_C$ shown by SPR (Fig. 2 and 3), these results are consistent with a mechanism

TABLE 1 Transcriptional analysis of the *agr* specificity of OHM

Focus	Gene	*agr* regulation/association	Fold change in gene expression (vehicle/OHM treatment)[a]			
			LAC	*P* value	Δ*agr*[b]	*P* value
Virulence	*spa* (SAUSA300_0113)	Neg	<2		ND	
	set7 (SAUSA300_0396)	NA[c]	−2.84	0.0019	<2	
	saeR (SAUSA300_0691)	Pos	<2		ND	
Stress response	*asp23* (SAUSA300_2142)	NA	<2		ND	
	crtM (SAUSA300_2499)	NA	<2		ND	
	clpB (SAUSA300_0877)	NA	<2		ND	
Metabolism	*atpG* (SAUSA300_2059)	NA	<2		ND	
	murQ (SAUSA300_0193)	Pos	−4.99	<0.0001	−8.551	<0.0001
	sdhA (SAUSA300_1047)	NA	<2		ND	
Efflux/antibiotic resistance	*norA* (SAUSA300_0680)	NA	<2		ND	
	mdrA (SAUSA300_2299)	NA	<2		ND	
	NaMDR gene[d] (SAUSA300_0335)	NA	−3.23	0.0015	−2.26	0.0076

[a] Values are shown if ≥2-fold.

[b] Assay performed with Δ*agr* strain if ≥2-fold difference with OHM treatment of LAC. ND, not done.

[c] NA, not applicable.

[d] NaMDR, Na$^+$-driven multidrug efflux pump.

whereby OHM predominantly functions as an inhibitor of *agr* activation.

ω-Hydroxyemodin attenuates *S. aureus* SSTI. Invasive *S. aureus* SSTIs require *agr*-regulated virulence factors (14, 19, 58–60). Therefore, we assessed the efficacy of OHM in an established mouse model of *S. aureus* SSTI (42). Over the course of a three-day infection with the USA300 isolate LAC, a single 5-μg dose of OHM administered at the time of infection significantly inhibited abscess (Fig. 4A and B) and ulcer (dermonecrosis) formation (Fig. 4A and C), as well as morbidity at day one postinfection (assessed by weight loss) compared to that of the vehicle-treated controls (Fig. 4D). In contrast, no differences were observed between the OHM and vehicle-treated mice infected with LACΔ*agr* (Fig. 4A and data not shown), demonstrating the specificity of OHM for disrupting *agr* signaling without directly impacting the host. Importantly, the single OHM treatment reduced the day three and day seven postinfection bacterial burden at the site of infection in LAC-infected (Fig. 4E) but not Δ*agr*-infected mice (Fig. 4F), suggesting that mice were better able to combat the infection in the absence of *agr* signaling.

We predicted that if OHM treatment supported host-mediated clearance by disrupting *agr* signaling, OHM-treated LAC, but not LACΔ*agr*, would be more readily killed by innate immune cells *in vitro* compared to in the vehicle-treated controls. As predicted, OHM treatment of LAC, but not LACΔ*agr*, resulted in significantly increased intracellular killing by both mouse macrophages (Fig. 5A) and human PMNs (Fig. 5B) compared to that in the vehicle-treated controls. This increased killing was not a result of OHM-mediated effects on opsonophagocytosis, as the total number of bacteria phagocytosed (see Fig. S5 in the supplemental material) and the percentage of bacteria phagocytosed relative to the total inoculum (data not shown) were equivalent, regardless of whether the bacteria were pretreated with vehicle or OHM. Furthermore, OHM treatment of LAC but not LACΔ*agr* protected human PMNs from killing by secreted *agr*-regulated virulence

factors. PMNs showed significantly increased survival in the presence of supernatant from OHM- versus vehicle-treated LAC (Fig. 5C). Together, these results demonstrate that OHM supports the host-mediated clearance of *S. aureus* by inhibiting *agr*-mediated virulence.

ω-Hydroxyemodin limits inflammation mediated by *S. aureus* QS. *S. aureus* uses a variety of virulence factors, many of which are regulated by the *agr* system, to evade host clearance mechanisms. These virulence factors cause tissue damage and inflammation and facilitate invasive infection (61–65). Therefore, we postulated that the reduction in bacterial burden in the LAC-infected, OHM-treated mice would be associated with reduced tissue damage and reduced local inflammatory cytokine production compared to the vehicle-treated controls. Histological analysis of day three postinfection skin sections confirmed the overall reduction in abscess formation and ulceration in OHM-treated mice (Fig. 6A). Additionally, skin sections from the vehicle-treated mice displayed a disorganized architecture at both the epithelium-to-necrosis transition (Fig. 6A, left inset) and the abscess periphery (right inset) compared to sections from OHM-treated mice. Also as predicted, OHM treatment resulted in a local cytokine profile matching that of LACΔ*agr*-infected mice on day three postinfection (Fig. 6B), with significant reductions in interleukin-1β (IL-1β), tumor necrosis factor alpha (TNF-α), and IL-6, but not the anti-inflammatory cytokine IL-10, compared to the vehicle-treated controls. LAC-infected mice treated with OHM also showed reduced transcription of *il-1*β, *tnf*α, and *il-6* at 24 h postinfection compared to the levels in the vehicle-treated mice (Fig. 6C). Finally, the activation of the NLRP3 inflammasome and the subsequent release of IL-1β is induced by pore formation in the host cell membranes by Hla (66–68), and the passive transfer of Hla-neutralizing antibodies is sufficient to limit the secretion of IL-1β (69). Therefore, we predicted that OHM treatment would be associated with reduced Hla expression and
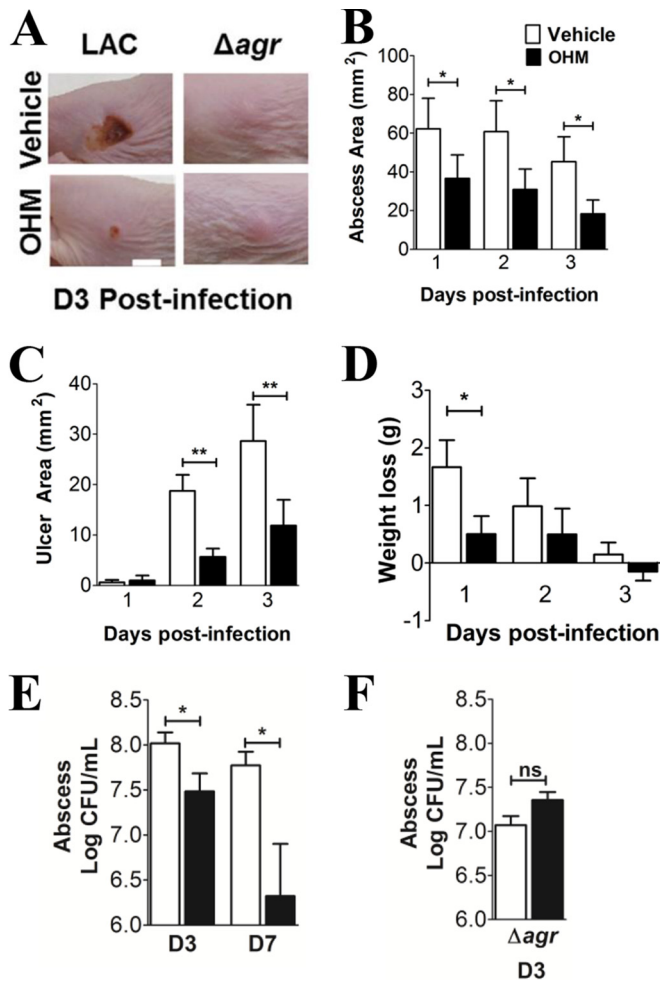
FIG 4 ω-Hydroxyemodin limits abscess formation and dermonecrosis and promotes bacterial clearance in a mouse model of *S. aureus* SSTI. SKH1 mice were subcutaneously injected with 5×10^7 to 7×10^7 CFU of LAC or Δ*agr* along with OHM (0.2 mg/kg) or vehicle control. (A) Representative images of abscesses and ulcers on day three postinfection (D3) (scale bar = 5 mm). Day 3 postinfection abscess (B), ulcer area (C), and weight loss of LAC-infected mice. (E) Day 3 and day 7 postinfection bacterial burden at the site of infection. The data shown are the mean ± SEM (LAC, day 3, *n* = 12 to 16 mice per group; day 7, *n* = 5 mice per group). (F) Δ*agr* day 3 bacterial burden at the site of infection. *n* = 6 mice per group. ns, not significant. *, $P < 0.05$; **, $P < 0.01$ by Mann-Whitney U test.

nlrp3 transcription at the site of infection. As expected, the OHM-treated mice showed decreased local Hla expression and decreased transcription of *nlrp3* compared to the vehicle-treated controls (Fig. 6D and E). Together, these data demonstrate that OHM inhibition of *agr* signaling limits host tissue damage and inflammation during *S. aureus* SSTI.

DISCUSSION

Recently, the National Institutes of Allergy and Infectious Diseases reported on the current status and future directions for its antibacterial resistance program (70). Two of the strategic approaches highlighted were (i) antivirulence strategies to disarm bacteria to reduce pathogenesis and (ii) approaches to harness the host immune system to better combat infections. Here, we report that OHM, a natural product isolated from the fungus *P. restrictum*
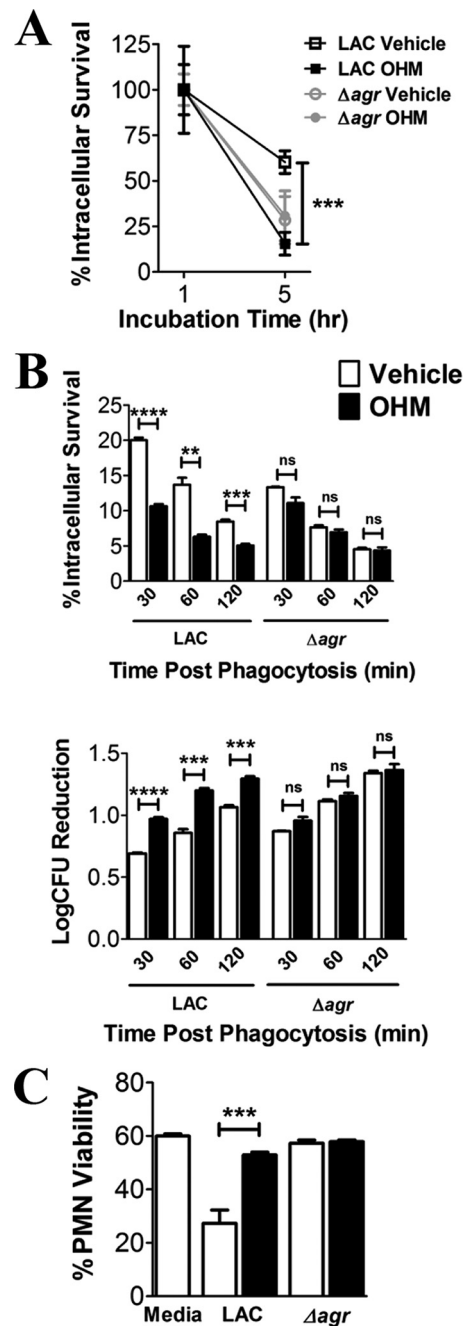

FIG 5 ω-Hydroxyemodin supports immune cell killing of *agr*+ *S. aureus*. (A) Mouse macrophage (RAW 264.7) intracellular killing of bacteria pretreated with OHM or vehicle control. The data are shown as the mean ± SEM normalized to 100% after 1 h of incubation at an MOI of 1:1. *n* = 6 from two independent experiments performed in triplicate. (B) Human polymorphonuclear leukocyte (PMN) intracellular killing of bacteria pretreated with OHM or vehicle control. The data are the mean ± SEM presented as the percent survival (top) and log CFU reduction (bottom) compared to time zero. (C) Supernatant lysis of human PMNs, assessed by LDH release, after 2 h of incubation with sterile supernatant from overnight cultures grown in the presence of OHM or vehicle control. The data are the mean ± SEM, presented as percent PMN viability compared to 100% lysis by Triton X-100. (B and C) Experiments were performed in triplicate with PMNs from two separate donors. A representative donor experiment is shown. ns, not significant. **, $P < 0.01$; ***, $P < 0.001$; ****, $P \leq 0.0001$ by Student's *t* test.
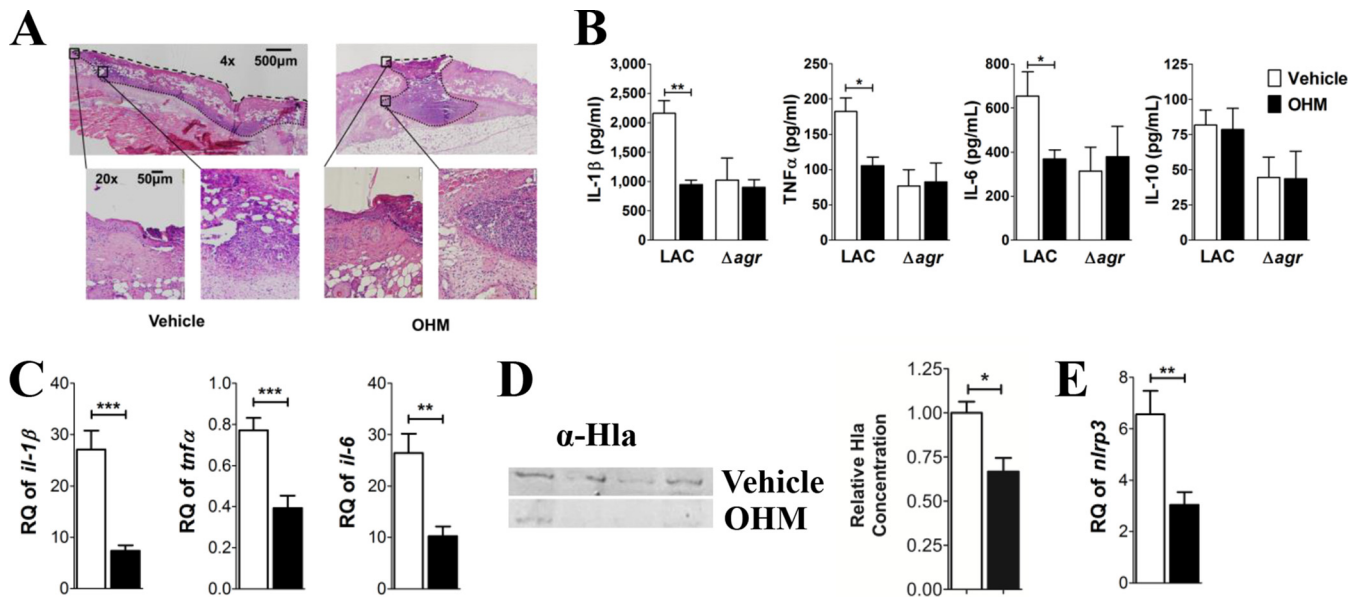
FIG 6 ω-Hydroxyemodin limits pathology and expression of inflammatory cytokines during *S. aureus* SSTI. (A) Top, representative hematoxylin and eosin micrographs of 5-μm sagittal sections of day three post-LAC infection abscess tissue. The abscess area is demarcated by a fine dashed line, while the ulcer surface length is marked by the thick dash line. Bottom, magnification of the transition from normal epithelium to necrotic tissue (left) and organization of the abscess tissue (right). (B) Multiplex analysis of cytokines present in the abscess tissue on day three postinfection with LAC or Δ*agr*. (C and E) Quantification of *il-1*β, *tnf*α, *il-6* (C), and *nlrp3* (E) relative to *hprt* in abscess tissue at 24 h post-LAC infection. (D) Western blot analysis and quantification of Hla at the site of infection (day 3) in OHM- versus vehicle-treated mice (*n* = 4 mice/group). The data are the mean ± SEM from infection data, as described in the legend to Fig. 4. RQ, relative quantification; *, *P* < 0.05; **, *P* < 0.01; ***, *P* < 0.001 by Student's *t* test.

(27), addresses both goals by directly inhibiting *S. aureus* QS-dependent virulence while indirectly bolstering the host immune response against *S. aureus* infection. In a mouse model of *S. aureus* SSTI, OHM significantly decreases abscess and ulcer formation and promotes bacterial clearance. Importantly, OHM treatment reduces tissue damage and limits local proinflammatory cytokine production to levels seen in mice infected with the *agr* deletion mutant. Furthermore, OHM treatment enhances immune cell-mediated killing of *S. aureus* in an *agr*-dependent manner. Therefore, these data demonstrate that antivirulence strategies can limit disease by disarming the bacteria while concurrently reducing inflammation and promoting host innate defense. In addition, this is the first polyhydroxyanthraquinone described with *in vivo* efficacy against MRSA infection, adding to the expanse of natural products with the potential to promote human health and advance antibiotic stewardship.

Numerous reviews have addressed the potential role of antivirulence strategies, including the disruption of QS, in combating the antimicrobial resistance crisis (4, 6, 7, 71–73). We chose to focus on the disruption of *agr* QS as an antivirulence approach to *S. aureus* SSTIs due to their predominance in *S. aureus* disease manifestations, as well as the established contribution of *agr* in facilitating these infections (11–14, 19). For example, *agr* deletion mutants (Δ*agr*) are less pathogenic and more readily cleared during SSTIs than are wild-type strains (14, 19), and host innate effectors that disrupt *agr* signaling limit disease in skin infection models (20–22). Importantly, the sterile supernatant from *agr*⁺ but not from *agr*-null *S. aureus* strains is sufficient to cause skin lesions similar to those in an active infection, definitively demonstrating the role of *agr*-regulated secreted virulence factors in skin pathogenesis (58). Here, we used OHM in a prophylactic admin-

istration model, similar to that previously reported for the administration of competing AIP or the passive transfer of monoclonal antibodies targeting AIP4 (24, 58), to demonstrate that small-molecule-mediated disruption of *agr* signaling *in vivo* results in an "*agr*-null-like" host inflammatory profile.

The disruption of *agr* signaling during SSTIs results in reduced bacterial burden at various time points postinfection (19, 25, 58, 60), suggesting that host-mediated bacterial clearance is more effective in the absence of QS. In support of this, we have shown here and elsewhere (25) that *agr* inhibitors enhance some mechanisms of innate immune bacterial clearance against *agr*⁺ *S. aureus*. The increased bacterial clearance likely results from inhibiting the expression of the *agr*-regulated secretome, which includes virulence factors that target host immune cells. Among these, the phenol-soluble modulins (PSMs) and Hla, in particular, contribute to abscess formation, dermonecrosis, and bacterial burden during SSTIs (59, 60, 74, 75). These toxins target a variety of cell types to suppress both innate and adaptive immunity (76). For example, *S. aureus* utilizes Hla to survive inside neutrophils and macrophages (45, 77–80) and to induce programmed cell death in T cells, B cells, and monocytes (81). In addition, Hla activates the NLRP3 inflammasome in a variety of cells, resulting in the release of the inflammatory cytokine IL-1β (67, 68, 82). Although neutrophils and IL-1β are needed for the ultimate clearance of *S. aureus* SSTI (83, 84), limiting inflammation caused by bacterial toxins clearly benefits the host.

Our molecular modeling studies positioned OHM near R218 of *S. aureus* AgrA. This residue, which is strictly conserved across multiple staphylococcal species (46), is required for *agr* function and contributes to AgrA binding to *agr* promoter DNA (38, 47). Although the potential exists for OHM to drive selection for an

alternative amino acid at residue 218, any such mutation would likely result in *agr* dysfunction. The selection for QS-deficient isolates is unlikely to be of significant benefit to the pathogen, as these isolates are severely attenuated, more readily cleared by host defenses, and less effective at initiating infection (19, 37, 60). However, while the residues directly involved in OHM binding have yet to be definitively demonstrated, the question of whether OHM can select for mutation of other residues in the predicted binding site that would prevent OHM function while retaining *agr* activity will require empirical determination.

Along with inhibiting *S. aureus agr* activation, OHM likewise inhibits *agr* signaling by *S. epidermidis*, an important member of the skin microbiome and also an opportunistic pathogen (85). *S. epidermidis agr* regulation drives the mechanisms of resistance to host innate defense (86), suggesting that OHM or related analogues might prove efficacious against *S. epidermidis* infections. However, in its role as a commensal, *S. epidermidis* appears to benefit the host by such means as competing with *S. aureus* for colonization and contributing to overall skin immunity (87–89). Additionally, AIP1 produced by *S. epidermidis* is cross-inhibitory to *S. aureus agr* types I to III *in vitro* (85, 90, 91). Therefore, it is unclear whether OHM-mediated perturbation of *S. epidermidis* QS, during treatment for *S. aureus* SSTI, might result in unwarranted complications, such as increased host-mediated clearance of *S. epidermidis* and/or the loss of potentially beneficial cross-inhibitory AIP. To address these possibilities, it will be important to experimentally determine the *in vivo* implications of disrupting QS in an *S. epidermidis*-colonized host on subsequent *S. aureus* skin infection.

As is the case with existing antimicrobials, QS inhibitors (QSIs) may not be a one-size-fits-all solution. Although SSTIs comprise the vast majority of *S. aureus* infections, this pathogen causes a variety of disease manifestations, including pneumonia, osteomyelitis, endocarditis, and bloodstream infections (BSI). This raises the question of whether the use of QSIs will be universally beneficial. The contribution of *agr* to *S. aureus* pathogenesis has largely been demonstrated in models of SSTIs and pneumonia (14, 19, 24, 92). In contrast, *agr* dysfunction has been associated with persistent bacteremia in hospitalized patients (83, 84), suggesting that QSIs would be best utilized to prevent *S. aureus* invasion prior to BSI. Likewise, the disruption of *agr* is associated with biofilm formation *in vitro* (85), potentially limiting the utility of QSIs for the treatment of infections involving implanted devices, as well as osteomyelitis and endocarditis. Whether OHM and other QSIs would contribute to staphylococcal biofilm formation *in vivo* will require investigation in appropriate animal models of infection. Overall, however, QSIs might be a critical part of the developing arsenal for combating antibiotic resistance either alone, as adjuncts to existing antibiotics, or along with potential vaccines or other approaches to augment host defense.

A substantial portion of the compounds used to fight infections have their origins in natural products (26). Despite clearly representing a wealth of bioactive molecules, natural products have received limited attention with respect to identifying specific inhibitors of *S. aureus* QS that are not bactericidal. To date, other natural products identified as *agr* inhibitors include (i) α-cyperone from the nut grass plant *Cyperus rotundus* (93), (ii) the fungal metabolite ambuic acid (94), and extracts from (iii) the goldenseal plant *Hydrastis canadensis* (95) and (iv) three Italian medicinal plants, *Ballota nigra*, *Castanea sativa*, and *Sambucus ebulus* (96).

Among these, OHM is the first to demonstrate *in vivo* efficacy against *S. aureus* QS. Therefore, we predict that targeted testing of structurally diverse natural products will continue to reveal a broad range of antivirulence molecules with the potential to support innate host defense mechanisms and to positively contribute to antibiotic stewardship.

ACKNOWLEDGMENTS

REFERENCES

1. **Spellberg B, Bartlett JG, Gilbert DN.** 2013. The future of antibiotics and resistance. N Engl J Med **368**:299–302. http://dx.doi.org/10.1056/NEJMp1215093.
2. **Nathan C.** 2012. Fresh approaches to anti-infective therapies. Sci Transl Med **4**:140sr142. http://dx.doi.org/10.1126/scitranslmed.3003081.
3. **Park B, Liu GY.** 2012. Targeting the host-pathogen interface for treatment of *Staphylococcus aureus* infection. Semin Immunopathol **34**:299–315. http://dx.doi.org/10.1007/s00281-011-0297-1.
4. **Rutherford ST, Bassler BL.** 2012. Bacterial quorum sensing: its role in virulence and possibilities for its control. Cold Spring Harb Perspect Med **2**:a012427. http://dx.doi.org/10.1101/cshperspect.a012427.
5. **Gray B, Hall P, Gresham H.** 2013. Targeting *agr*- and *agr*-like quorum sensing systems for development of common therapeutics to treat multiple Gram-positive bacterial infections. Sensors **13**:5130–5166. http://dx.doi.org/10.3390/s130405130.
6. **Rasko DA, Sperandio V.** 2010. Anti-virulence strategies to combat bacteria-mediated disease. Nat Rev Drug Discov **9**:117–128. http://dx.doi.org/10.1038/nrd3013.
7. **Zhu J, Kaufmann GF.** 2013. Quo vadis quorum quenching? Curr Opin Pharmacol **13**:688–698. http://dx.doi.org/10.1016/j.coph.2013.07.003.
8. **Rampioni G, Leoni L, Williams P.** 2014. The art of antibacterial warfare: deception through interference with quorum sensing-mediated communication. Bioorg Chem **55**:60–68. http://dx.doi.org/10.1016/j.bioorg.2014.04.005.
9. **Harraghy N, Kerdudou S, Herrmann M.** 2007. Quorum-sensing systems in staphylococci as therapeutic targets. Anal Bioanal Chem **387**:437–444. http://dx.doi.org/10.1007/s00216-006-0860-0.
10. **Cegelski L, Marshall GR, Eldridge GR, Hultgren SJ.** 2008. The biology and future prospects of antivirulence therapies. Nat Rev Microbiol **6**:17–27. http://dx.doi.org/10.1038/nrmicro1818.
11. **Moran GJ, Krishnadasan A, Gorwitz RJ, Fosheim GE, McDougal LK, Carey RB, Talan DA,** EMERGEncy ID Net Study Group. 2006. Methicillin-resistant *S. aureus* infections among patients in the emergency department. N Engl J Med **355**:666–674. http://dx.doi.org/10.1056/NEJMoa055356.
12. **Lowy FD.** 1998. *Staphylococcus aureus* infections. N Engl J Med **339**:520–532. http://dx.doi.org/10.1056/NEJM199808203390806.
13. **Tong SY, Chen LF, Fowler VG.** 2012. Colonization, pathogenicity, host susceptibility, and therapeutics for *Staphylococcus aureus*: what is the clinical relevance? Semin Immunopathol **34**:185–200. http://dx.doi.org/10.1007/s00281-011-0300-x.
14. **Cheung GY, Wang R, Khan BA, Sturdevant DE, Otto M.** 2011. Role of the accessory gene regulator *agr* in community-associated methicillin-resistant *Staphylococcus aureus* pathogenesis. Infect Immun **79**:1927–1935. http://dx.doi.org/10.1128/IAI.00046-11.
15. **Novick RP, Geisinger E.** 2008. Quorum sensing in staphylococci. Annu Rev Genet **42**:541–564. http://dx.doi.org/10.1146/annurev.genet.42.110807.091640.
16. **Thoendel M, Kavanaugh JS, Flack CE, Horswill AR.** 2011. Peptide signaling in the staphylococci. Chem Rev **111**:117–151. http://dx.doi.org/10.1021/cr100370n.
17. **Jacobsson G, Gustafsson E, Andersson R.** 2008. Outcome for invasive

Staphylococcus aureus infections. Eur J Clin Microbiol Infect Dis **27**:839–848. http://dx.doi.org/10.1007/s10096-008-0515-5.

18. **Jarraud S, Mougel C, Thioulouse J, Lina G, Meugnier H, Forey F, Nesme X, Etienne J, Vandenesch F.** 2002. Relationships between *Staphylococcus aureus* genetic background, virulence factors, *agr* groups (alleles), and human disease. Infect Immun **70**:631–641. http://dx.doi.org/10.1128/IAI.70.2.631-641.2002.

19. **Montgomery CP, Boyle-Vavra S, Daum RS.** 2010. Importance of the global regulators *agr* and SaeRS in the pathogenesis of CA-MRSA USA300 infection. PLoS One **5**:e15177. http://dx.doi.org/10.1371/journal.pone.0015177.

20. **Rothfork JM, Timmins GS, Harris MN, Chen X, Lusis AJ, Otto M, Cheung AL, Gresham HD.** 2004. Inactivation of a bacterial virulence pheromone by phagocyte-derived oxidants: new role for the NADPH oxidase in host defense. Proc Natl Acad Sci U S A **101**:13867–13872. http://dx.doi.org/10.1073/pnas.0402996101.

21. **Hall PR, Elmore BO, Spang CH, Alexander SM, Manifold-Wheeler BC, Castleman MJ, Daly SM, Peterson MM, Sully EK, Femling JK, Otto M, Horswill AR, Timmins GS, Gresham HD.** 2013. Nox2 modification of LDL is essential for optimal apolipoprotein B-mediated control of *agr* type III *Staphylococcus aureus* quorum-sensing. PLoS Pathog **9**:e1003166. http://dx.doi.org/10.1371/journal.ppat.1003166.

22. **Nishimura H, Mayama M, Komatsu Y, Kato H, Shimaoka N, Tanaka Y.** 1964. Showdomycin, a new antibiotic from a *Streptomyces* sp. J Antibiot (Tokyo) **17**:148–155.

23. **Schlievert PM, Case LC, Nemeth KA, Davis CC, Sun Y, Qin W, Wang F, Brosnahan AJ, Mleziva JA, Peterson ML, Jones BE.** 2007. Alpha and beta chains of hemoglobin inhibit production of *Staphylococcus aureus* exotoxins. Biochemistry **46**:14349–14358. http://dx.doi.org/10.1021/bi701202w.

24. **Park J, Jagasia R, Kaufmann GF, Mathison JC, Ruiz DI, Moss JA, Meijler MM, Ulevitch RJ, Janda KD.** 2007. Infection control by antibody disruption of bacterial quorum sensing signaling. Chem Biol **14**:1119–1127. http://dx.doi.org/10.1016/j.chembiol.2007.08.013.

25. **Sully EK, Malachowa N, Elmore BO, Alexander SM, Femling JK, Gray BM, DeLeo FR, Otto M, Cheung AL, Edwards BS, Sklar LA, Horswill AR, Hall PR, Gresham HD.** 2014. Selective chemical inhibition of *agr* quorum sensing in *Staphylococcus aureus* promotes host defense with minimal impact on resistance. PLoS Pathog **10**:e1004174. http://dx.doi.org/10.1371/journal.ppat.1004174.

26. **Newman DJ, Cragg GM.** 2012. Natural products as sources of new drugs over the 30 years from 1981 to 2010. J Nat Prod **75**:311–335. http://dx.doi.org/10.1021/np200906s.

27. **Figueroa M, Jarmusch AK, Raja HA, El-Elimat T, Kavanaugh JS, Horswill AR, Cooks RG, Cech NB, Oberlies NH.** 2014. Polyhydroxyanthraquinones as quorum sensing inhibitors from the guttates of *Penicillium restrictum* and their analysis by desorption electrospray ionization mass spectrometry. J Nat Prod **77**:1351–1358. http://dx.doi.org/10.1021/np5000704.

28. **Malone CL, Boles BR, Lauderdale KJ, Thoendel M, Kavanaugh JS, Horswill AR.** 2009. Fluorescent reporters for *Staphylococcus aureus*. J Microbiol Methods **77**:251–260. http://dx.doi.org/10.1016/j.mimet.2009.02.011.

29. **Olson ME, Todd DA, Schaeffer CR, Paharik AE, Van Dyke MJ, Buttner H, Dunman PM, Rohde H, Cech NB, Fey PD, Horswill AR.** 2014. *Staphylococcus epidermidis agr* quorum-sensing system: signal identification, cross talk, and importance in colonization. J Bacteriol **196**:3482–3493. http://dx.doi.org/10.1128/JB.01882-14.

30. **Rothfork JM, Dessus-Babus S, Wamel WJV, Cheung AL, Gresham HD.** 2003. Fibrinogen depletion attenuates *Staphylococcus aureus* infection by preventing density-dependent virulence gene up-regulation. J Immunol **171**:5389–5395. http://dx.doi.org/10.4049/jimmunol.171.10.5389.

31. **Bernheimer AW.** 1988. Assay of hemolytic toxins. Methods Enzymol **165**:213–217. http://dx.doi.org/10.1016/S0076-6879(88)65033-6.

32. **Corrigan RM, Foster TJ.** 2009. An improved tetracycline-inducible expression vector for *Staphylococcus aureus*. Plasmid **61**:126–129. http://dx.doi.org/10.1016/j.plasmid.2008.10.001.

33. **Geisinger E, Muir TW, Novick RP.** 2009. *agr* receptor mutants reveal distinct modes of inhibition by staphylococcal autoinducing peptides. Proc Natl Acad Sci U S A **106**:1216–1221. http://dx.doi.org/10.1073/pnas.0807760106.

34. **Fey PD, Endres JL, Yajjala VK, Widhelm TJ, Boissy RJ, Bose JL, Bayles KW.** 2013. A genetic resource for rapid and comprehensive phenotype

35. **Luong TT, Lee CY.** 2007. Improved single-copy integration vectors for *Staphylococcus aureus*. J Microbiol Methods **70**:186–190. http://dx.doi.org/10.1016/j.mimet.2007.04.007.

36. **Scudiero DA, Shoemaker RH, Paull KD, Monks A, Tierney S, Nofziger TH, Currens MJ, Seniff D, Boyd MR.** 1988. Evaluation of a soluble tetrazolium formazan assay for cell-growth and drug sensitivity in culture using human and other tumor-cell lines. Cancer Res **48**:4827–4833.

37. **Sun F, Liang H, Kong X, Xie S, Cho H, Deng X, Ji Q, Zhang H, Alvarez S, Hicks LM, Bae T, Luo C, Jiang H, He C.** 2012. Quorum-sensing *agr* mediates bacterial oxidation response via an intramolecular disulfide redox switch in the response regulator AgrA. Proc Natl Acad Sci U S A **109**:9095–9100. http://dx.doi.org/10.1073/pnas.1200603109.

38. **Sidote DJ, Barbieri CM, Wu T, Stock AM.** 2008. Structure of the *Staphylococcus aureus* AgrA LytTR domain bound to DNA reveals a beta fold with an unusual mode of binding. Structure **16**:727–735. http://dx.doi.org/10.1016/j.str.2008.02.011.

39. **Trott O, Olson AJ.** 2010. AutoDock Vina: improving the speed and accuracy of docking with a new scoring function, efficient optimization, and multithreading. J Comput Chem **31**:455–461. http://dx.doi.org/10.1002/jcc.21334.

40. **Leonard PG, Bezar IF, Sidote DJ, Stock AM.** 2012. Identification of a hydrophobic cleft in the LytTR domain of AgrA as a locus for small molecule interactions that inhibit DNA binding. Biochemistry **51**:10035–10043. http://dx.doi.org/10.1021/bi3011785.

41. **Berman HM, Westbrook J, Feng Z, Gilliland G, Bhat TN, Weissig H, Shindyalov IN, Bourne PE.** 2000. The Protein Data Bank. Nucleic Acids Res **28**:235–242. http://dx.doi.org/10.1093/nar/28.1.235.

42. **Malachowa N, Kobayashi SD, Braughton KR, DeLeo FR.** 2013. Mouse model of *Staphylococcus aureus* skin infection. Methods Mol Biol **1031**:109–116. http://dx.doi.org/10.1007/978-1-62703-481-4_14.

43. **Schneider CA, Rasband WS, Eliceiri KW.** 2012. NIH Image to ImageJ: 25 years of image analysis. Nat Methods **9**:671–675. http://dx.doi.org/10.1038/nmeth.2089.

44. **Nauseef WM.** 2014. Isolation of human neutrophils from venous blood. Methods Mol Biol **1124**:13–18. http://dx.doi.org/10.1007/978-1-62703-845-4_2.

45. **Pang YY, Schwartz J, Thoendel M, Ackermann LW, Horswill AR, Nauseef WM.** 2010. *agr*-dependent interactions of *Staphylococcus aureus* USA300 with human polymorphonuclear neutrophils. J Innate Immun **2**:546–559. http://dx.doi.org/10.1159/000319855.

46. **Nicod SS, Weinzierl RO, Burchell L, Escalera-Maurer A, James EH, Wigneshwararaj S.** 2014. Systematic mutational analysis of the LytTR DNA binding domain of *Staphylococcus aureus* virulence gene transcription factor AgrA. Nucleic Acids Res **42**:12523–12536. http://dx.doi.org/10.1093/nar/gku1015.

47. **Shopsin B, Eaton C, Wasserman GA, Mathema B, Adhikari RP, Agolory S, Altman DR, Holzman RS, Kreiswirth BN, Novick RP.** 2010. Mutations in *agr* do not persist in natural populations of methicillin-resistant *Staphylococcus aureus*. J Infect Dis **202**:1593–1599. http://dx.doi.org/10.1086/656915.

48. **Dunman PM, Murphy E, Haney S, Palacios D, Tucker-Kellogg G, Wu S, Brown EL, Zagursky RJ, Shlaes D, Projan SJ.** 2001. Transcription profiling-based identification of *Staphylococcus aureus* genes regulated by the *agr* and/or *sarA* loci. J Bacteriol **183**:7341–7353. http://dx.doi.org/10.1128/JB.183.24.7341-7353.2001.

49. **Nagarajan V, Smeltzer MS, Elasri MO.** 2009. Genome-scale transcriptional profiling in *Staphylococcus aureus*: bringing order out of chaos. FEMS Microbiol Lett **295**:204–210. http://dx.doi.org/10.1111/j.1574-6968.2009.01595.x.

50. **Cirz RT, Jones MB, Gingles NA, Minogue TD, Jarrahi B, Peterson SN, Romesberg FE.** 2007. Complete and SOS-mediated response of *Staphylococcus aureus* to the antibiotic ciprofloxacin. J Bacteriol **189**:531–539. http://dx.doi.org/10.1128/JB.01464-06.

51. **Baker J, Sitthisak S, Sengupta M, Johnson M, Jayaswal RK, Morrissey JA.** 2010. Copper stress induces a global stress response in *Staphylococcus aureus* and represses *sae* and *agr* expression and biofilm formation. Appl Environ Microbiol **76**:150–160. http://dx.doi.org/10.1128/AEM.02268-09.

52. **Dengler V, Meier PS, Heusser R, Berger-Bachi B, McCallum N.** 2011. Induction kinetics of the *Staphylococcus aureus* cell wall stress stimulon in

response to different cell wall active antibiotics. BMC Microbiol **11:**16. http://dx.doi.org/10.1186/1471-2180-11-16.

53. **Reiss S, Pane-Farre J, Fuchs S, Francois P, Liebeke M, Schrenzel J, Lindequist U, Lalk M, Wolz C, Hecker M, Engelmann S.** 2012. Global analysis of the *Staphylococcus aureus* response to mupirocin. Antimicrob Agents Chemother **56:**787–804. http://dx.doi.org/10.1128/AAC.05363-11.

54. **Song Y, Lunde CS, Benton BM, Wilkinson BJ.** 2012. Further insights into the mode of action of the lipoglycopeptide telavancin through global gene expression studies. Antimicrob Agents Chemother **56:**3157–3164. http://dx.doi.org/10.1128/AAC.05403-11.

55. **Reith J, Mayer C.** 2011. Peptidoglycan turnover and recycling in Gram-positive bacteria. Appl Microbiol Biotechnol **92:**1–11. http://dx.doi.org/10.1007/s00253-011-3486-x.

56. **Jaeger T, Mayer C.** 2008. *N*-acetylmuramic acid 6-phosphate lyases (MurNAc etherases): role in cell wall metabolism, distribution, structure, and mechanism. Cell Mol Life Sci **65:**928–939. http://dx.doi.org/10.1007/s00018-007-7399-x.

57. **Hadi T, Hazra S, Tanner ME, Blanchard JS.** 2013. Structure of MurNAc 6-phosphate hydrolase (MurQ) from *Haemophilus influenzae* with a bound inhibitor. Biochemistry **52:**9358–9366. http://dx.doi.org/10.1021/bi4010446.

58. **Wright JS, III, Jin R, Novick RP.** 2005. Transient interference with staphylococcal quorum sensing blocks abscess formation. Proc Natl Acad Sci U S A **102:**1691–1696. http://dx.doi.org/10.1073/pnas.0407661102.

59. **Wang R, Braughton KR, Kretschmer D, Bach THL, Queck SY, Li M, Kennedy AD, Dorward DW, Klebanoff SJ, Peschel A, Deleo FR, Otto M.** 2007. Identification of novel cytolytic peptides as key virulence determinants for community-associated MRSA. Nat Med **13:**1510–1514. http://dx.doi.org/10.1038/nm1656.

60. **Kobayashi SD, Malachowa N, Whitney AR, Braughton KR, Gardner DJ, Long D, Bubeck Wardenburg J, Schneewind O, Otto M, Deleo FR.** 2011. Comparative analysis of USA300 virulence determinants in a rabbit model of skin and soft tissue infection. J Infect Dis **204:**937–941. http://dx.doi.org/10.1093/infdis/jir441.

61. **Anwar S, Prince LR, Foster SJ, Whyte MK, Sabroe I.** 2009. The rise and rise of *Staphylococcus aureus*: laughing in the face of granulocytes. Clin Exp Immunol **157:**216–224. http://dx.doi.org/10.1111/j.1365-2249.2009.03950.x.

62. **Foster TJ.** 2005. Immune evasion by staphylococci. Nat Rev Microbiol **3:**948–958. http://dx.doi.org/10.1038/nrmicro1289.

63. **Zecconi A, Scali F.** 2013. *Staphylococcus aureus* virulence factors in evasion from innate immune defenses in human and animal diseases. Immunol Lett **150:**12–22. http://dx.doi.org/10.1016/j.imlet.2013.01.004.

64. **Diep BA, Otto M.** 2008. The role of virulence determinants in community-associated MRSA pathogenesis. Trends Microbiol **16:**361–369. http://dx.doi.org/10.1016/j.tim.2008.05.002.

65. **Gordon RJ, Lowy FD.** 2008. Pathogenesis of methicillin-resistant *Staphylococcus aureus* infection. Clin Infect Dis **46**(Suppl 5)**:**S350–S359. http://dx.doi.org/10.1086/533591.

66. **Berube BJ, Wardenburg JB.** 2013. *Staphylococcus aureus* α-toxin: nearly a century of intrigue. Toxins (Basel) **5:**1140–1166. http://dx.doi.org/10.3390/toxins5061140.

67. **Muñoz-Planillo R, Franchi L, Miller LS, Nuñez G.** 2009. A critical role for hemolysins and bacterial lipoproteins in *Staphylococcus aureus*-induced activation of the Nlrp3 inflammasome. J Immunol **183:**3942–3948. http://dx.doi.org/10.4049/jimmunol.0900729.

68. **Craven RR, Gao X, Allen IC, Gris D, Bubeck Wardenburg J, McElvania-Tekippe E, Ting JP, Duncan JA.** 2009. *Staphylococcus aureus* alpha-hemolysin activates the NLRP3-inflammasome in human and mouse monocytic cells. PLoS One **4:**e7446. http://dx.doi.org/10.1371/journal.pone.0007446.

69. **Bubeck Wardenburg J, Schneewind O.** 2008. Vaccine protection against *Staphylococcus aureus* pneumonia. J Exp Med **205:**287–294. http://dx.doi.org/10.1084/jem.20072208.

70. **National Institute of Allergy and Infectious Diseases.** 2014. NIAID's antibacterial resistance program: current status and future directions. National Institute of Allergy and Infectious Diseases, Bethesda, MD. http://www.niaid.nih.gov/topics/antimicrobialresistance/documents/arstrategicplan2014.pdf.

71. **Cech NB, Horswill AR.** 2013. Small-molecule quorum quenchers to prevent *Staphylococcus aureus* infection. Future Microbiol **8:**1511–1514. http://dx.doi.org/10.2217/fmb.13.134.

72. **Kaufmann GF, Park J, Janda KD.** 2008. Bacterial quorum sensing: a new target for anti-infective immunotherapy. Expert Opin Biol Ther **8:**719–724. http://dx.doi.org/10.1517/14712598.8.6.719.

73. **Njoroge J, Sperandio V.** 2009. Jamming bacterial communication: new approaches for the treatment of infectious diseases. EMBO Mol Med **1:**201–210. http://dx.doi.org/10.1002/emmm.200900032.

74. **Kennedy AD, Bubeck Wardenburg J, Gardner DJ, Long D, Whitney AR, Braughton KR, Schneewind O, DeLeo FR.** 2010. Targeting of alpha-hemolysin by active or passive immunization decreases severity of USA300 skin infection in a mouse model. J Infect Dis **202:**1050–1058. http://dx.doi.org/10.1086/656043.

75. **Sampedro GR, DeDent AC, Becker RE, Berube BJ, Gebhardt MJ, Cao H, Bubeck Wardenburg J.** 2014. Targeting *Staphylococcus aureus* alpha-toxin as a novel approach to reduce severity of recurrent skin and soft-tissue infections. J Infect Dis **210:**1012–1018. http://dx.doi.org/10.1093/infdis/jiu223.

76. **Tkaczyk C, Hamilton MM, Datta V, Yang XP, Hilliard JJ, Stephens GL, Sadowska A, Hua L, O'Day T, Suzich J, Stover CK, Sellman BR.** 2013. *Staphylococcus aureus* alpha toxin suppresses effective innate and adaptive immune responses in a murine dermonecrosis model. PLoS One **8:**e75103. http://dx.doi.org/10.1371/journal.pone.0075103.

77. **Gresham HD, Lowrance JH, Caver TE, Wilson BS, Cheung AL, Lindberg FP.** 2000. Survival of *Staphylococcus aureus* inside neutrophils contributes to infection. J Immunol **164:**3713–3722. http://dx.doi.org/10.4049/jimmunol.164.7.3713.

78. **Voyich JA, Braughton KR, Sturdevant DE, Whitney AR, Said-Salim B, Porcella SF, Long RD, Dorward DW, Gardner DJ, Kreiswirth BN, Musser JM, DeLeo FR.** 2005. Insights into mechanisms used by *Staphylococcus aureus* to avoid destruction by human neutrophils. J Immunol **175:**3907–3919. http://dx.doi.org/10.4049/jimmunol.175.6.3907.

79. **Greenlee-Wacker MC, Rigby KM, Kobayashi SD, Porter AR, DeLeo FR, Nauseef WM.** 2014. Phagocytosis of *Staphylococcus aureus* by human neutrophils prevents macrophage efferocytosis and induces programmed necrosis. J Immunol **192:**4709–4717. http://dx.doi.org/10.4049/jimmunol.1302692.

80. **Kubica M, Guzik K, Koziel J, Zarebski M, Richter W, Gajkowska B, Golda A, Maciag-Gudowska A, Brix K, Shaw L, Foster T, Potempa J.** 2008. A potential new pathway for *Staphylococcus aureus* dissemination: the silent survival of *S. aureus* phagocytosed by human monocyte-derived macrophages. PLoS One **3:**e1409. http://dx.doi.org/10.1371/journal.pone.0001409.

81. **Nygaard TK, Pallister KB, DuMont AL, DeWald M, Watkins RL, Pallister EQ, Malone C, Griffith S, Horswill AR, Torres VJ, Voyich JM.** 2012. Alpha-toxin induces programmed cell death of human T cells, B cells, and monocytes during USA300 infection. PLoS One **7:**e36532. http://dx.doi.org/10.1371/journal.pone.0036532.

82. **Cho JS, Guo Y, Ramos RI, Hebroni F, Plaisier SB, Xuan C, Granick JL, Matsushima H, Takashima A, Iwakura Y, Cheung AL, Cheng G, Lee DJ, Simon SI, Miller LS.** 2012. Neutrophil-derived IL-1β is sufficient for abscess formation in immunity against *Staphylococcus aureus* in mice. PLoS Pathog **8:**e1003047. http://dx.doi.org/10.1371/journal.ppat.1003047.

83. **Rigby KM, DeLeo FR.** 2012. Neutrophils in innate host defense against *Staphylococcus aureus* infections. Semin Immunopathol **34:**237–259. http://dx.doi.org/10.1007/s00281-011-0295-3.

84. **Miller LS, Pietras EM, Uricchio LH, Hirano K, Rao S, Lin H, O'Connell RM, Iwakura Y, Cheung AL, Cheng G, Modlin RL.** 2007. Inflammasome-mediated production of IL-1beta is required for neutrophil recruitment against *Staphylococcus aureus* in vivo. J Immunol **179:**6933–6942. http://dx.doi.org/10.4049/jimmunol.179.10.6933.

85. **Otto M.** 2012. Molecular basis of *Staphylococcus epidermidis* infections. Semin Immunopathol **34:**201–214. http://dx.doi.org/10.1007/s00281-011-0296-2.

86. **Yao Y, Vuong C, Kocianova S, Villaruz AE, Lai Y, Sturdevant DE, Otto M.** 2006. Characterization of the *Staphylococcus epidermidis* accessory-gene regulator response: quorum-sensing regulation of resistance to human innate host defense. J Infect Dis **193:**841–848. http://dx.doi.org/10.1086/500246.

87. **Lina G, Boutite F, Tristan A, Bes M, Etienne J, Vandenesch F.** 2003. Bacterial competition for human nasal cavity colonization: role of staphylococcal *agr* alleles. Appl Environ Microbiol **69:**18–23. http://dx.doi.org/10.1128/AEM.69.1.18-23.2003.

88. **Naik S, Bouladoux N, Wilhelm C, Molloy MJ, Salcedo R, Kastenmuller W, Deming C, Quinones M, Koo L, Conlan S, Spencer S, Hall JA,**

Dzutsev A, Kong H, Campbell DJ, Trinchieri G, Segre JA, Belkaid Y. 2012. Compartmentalized control of skin immunity by resident commensals. Science **337:**1115–1119. http://dx.doi.org/10.1126/science.1225152.

89. Nakamizo S, Egawa G, Honda T, Nakajima S, Belkaid Y, Kabashima K. 2015. Commensal bacteria and cutaneous immunity. Semin Immunopathol **37:**73–80. http://dx.doi.org/10.1007/s00281-014-0452-6.

90. Otto M, Echner H, Voelter W, Gotz F. 2001. Pheromone cross-inhibition between *Staphylococcus aureus* and *Staphylococcus epidermidis*. Infect Immun **69:**1957–1960. http://dx.doi.org/10.1128/IAI.69.3.1957-1960.2001.

91. Otto M, Sussmuth R, Vuong C, Jung G, Gotz F. 1999. Inhibition of virulence factor expression in *Staphylococcus aureus* by the *Staphylococcus epidermidis agr* pheromone and derivatives. FEBS Lett **450:**257–262. http://dx.doi.org/10.1016/S0014-5793(99)00514-1.

92. Wright, JS, III, Jin R, Novick RP. 2005. Transient interference with staphylococcal quorum sensing blocks abscess formation. Proc Natl Acad Sci U S A **102:**1691–1696. http://dx.doi.org/10.1073/pnas.0407661102.

93. Luo M, Qiu J, Zhang Y, Wang J, Dong J, Li H, Leng B, Zhang Q, Dai X, Niu X, Zhao S, Deng X. 2012. α-Cyperone alleviates lung cell injury caused by *Staphylococcus aureus* via attenuation of alpha-hemolysin expression. J Microbiol Biotechnol **22:**1170–1176. http://dx.doi.org/10.4014/jmb.1202.02017.

94. Nakayama J, Uemura Y, Nishiguchi K, Yoshimura N, Igarashi Y, Sonomoto K. 2009. Ambuic acid inhibits the biosynthesis of cyclic peptide quormones in Gram-positive bacteria. Antimicrob Agents Chemother **53:**580–586. http://dx.doi.org/10.1128/AAC.00995-08.

95. Cech NB, Junio HA, Ackermann LW, Kavanaugh JS, Horswill AR. 2012. Quorum quenching and antimicrobial activity of goldenseal (*Hydrastis canadensis*) against methicillin-resistant *Staphylococcus aureus* (MRSA). Planta Med **78:**1556–1561. http://dx.doi.org/10.1055/s-0032-1315042.

96. Quave CL, Plano LR, Bennett BC. 2011. Quorum sensing inhibitors of *Staphylococcus aureus* from Italian medicinal plants. Planta Med **77:**188–195. http://dx.doi.org/10.1055/s-0030-1250145.

97. National Research Council. 2011. Guide for the care and use of laboratory animals: 8th ed. National Academies Press, Washington, DC.